

Supporting Information

Handy imaging sensor array based on the phase transformation from
CsPbBr₃ to CsPb₂Br₅: high sensitivity and rapid detection of water
content in ethanol

Rongmeng Gu,^a Xiuting Li,^{*b} Yan Meng,^c Zihui Li,^d Hongyu Nie,^d Xiaokun Wang^a and Dan Xiao^{*a,c,d}

^a College of Chemical Engineering, Sichuan University, Chengdu 610065, China. Email: xiaodan@scu.edu.cn

^b Institute for Advanced Study, Shenzhen University, Shenzhen 518060, China. Email: xiuting.li@szu.edu.cn

^c Institute of New Energy and Low-Carbon Technology, Sichuan University, Chengdu 610064, China.

^d College of Chemistry, Sichuan University, Chengdu 610064, China.

It can be seen that the diffraction pattern of F CsPbBr₃@PVA kept the typical lines of CsPbBr₃ (the lattice planes 100, 110 and 200), indicating the crystal structure of CsPbBr₃ still existed when CsPbBr₃ and PVA mixed shortly.

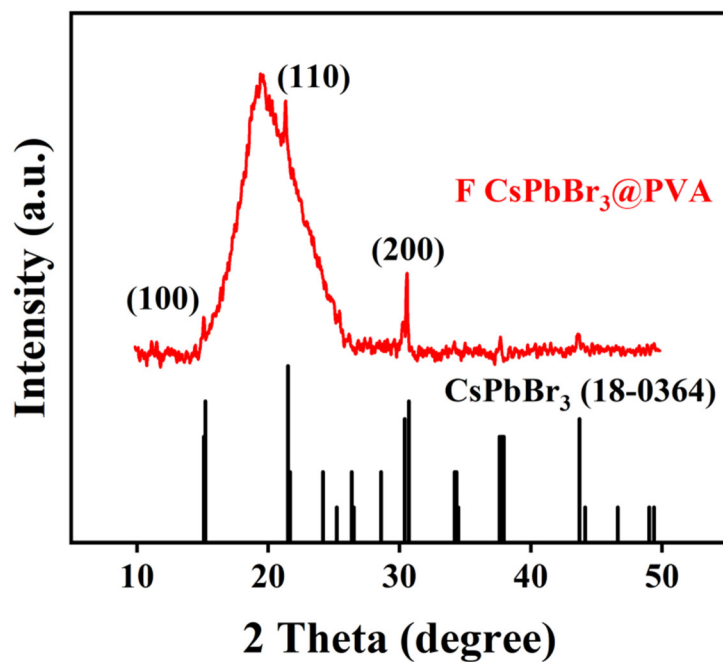


Figure S1. XRD of F CsPbBr₃@PVA (red), the standard CsPbBr₃ (black) obtained from the NO.18-0364 standard card.

The PLQY, defined as the percentage of photons emitted over photons absorbed by the sample, was determined by using an integrating sphere. A direct measurement was performed to measure PLQY of F CsPbBr₃@PVA and R CsPbBr₃@PVA. Emission spectra measured using fluorescence photometer with an integrating sphere attachment are provided as follows.

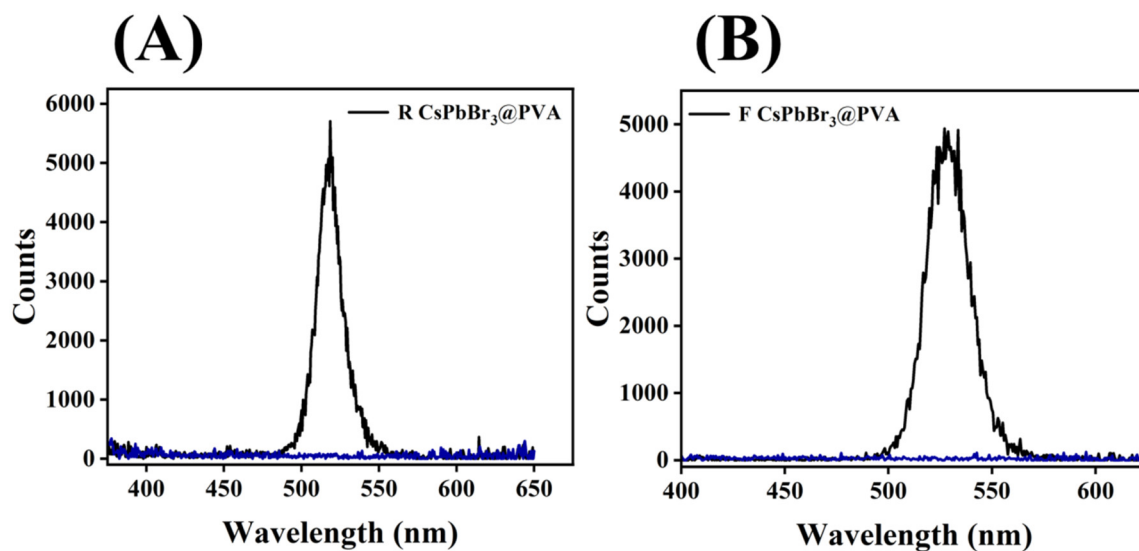


Figure S2. Determination of PLQY using integrating spheres: Emission spectra of R CsPbBr₃@PVA (A); Emission spectra of F CsPbBr₃@PVA (B).

The PL performances of CsPbBr₃@PVA degraded extensively with the extension of mixing time of CsPbBr₃ and PVA, and almost disappeared at 32 h.

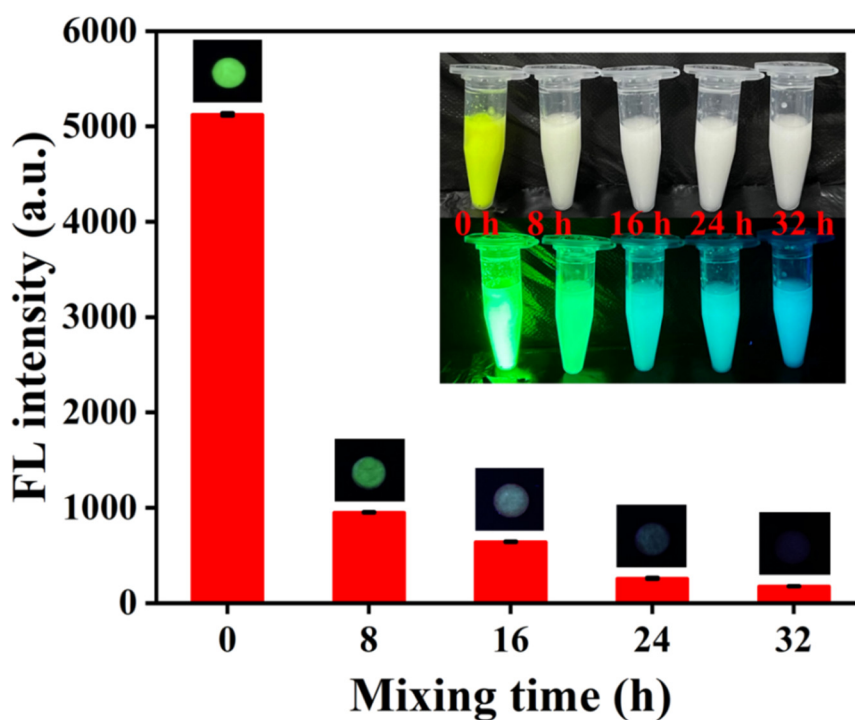


Figure S3. FL intensity of CsPbBr₃@PVA at different mixing time, insets on the upper right show the pictures of CsPbBr₃@PVA under room light (top) and 365 nm UV excitation (bottom), insets on the bar chart show the pictures of corresponding CsPbBr₃@PVA loaded on black wafers under 365 nm UV excitation.

The broad OH stretching vibration of the water and PVA molecules around 3300 cm^{-1} weakening after adding anhydrous ethanol to Q CsPbBr₃@PVA film, which shows evaporation of partial water molecules after anhydrous ethanol treatment.

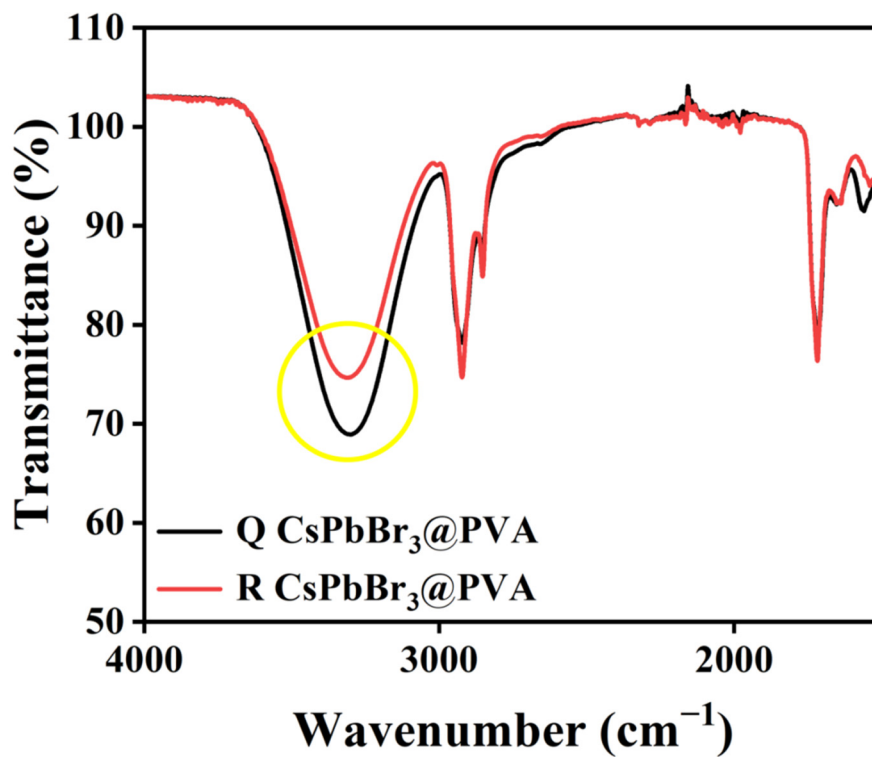


Figure S4. FT-IR spectra of Q CsPbBr₃@PVA (black) and R CsPbBr₃@PVA (red).

Q CsPbBr₃@PVA film was heated at 100 ° C for 1h to evaporate water molecules, and the recovery of green fluorescence was also observed, which proves the positive effect of water removal on the recrystallization of CsPb₂Br₅. The fluorescence of ethanol-treated Q CsPbBr₃@PVA (R CsPbBr₃@PVA) can be regenerated within a few seconds, indicating that the volatilization process accelerated by ethanol leads to the quick recrystallization and hence the recovery of green fluorescence.

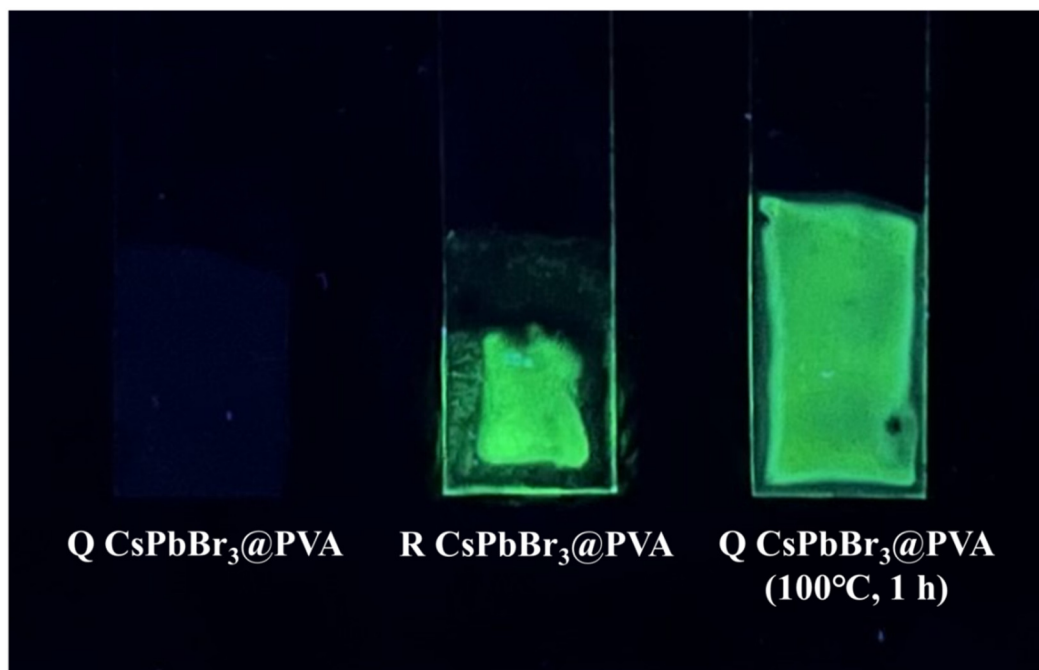


Figure S5. The photos of Q CsPbBr₃@PVA, R CsPbBr₃@PVA and Q CsPbBr₃@PVA after thermal treatment at 100 ° C for 1h under 365 nm UV light.

The gray-level image and 3D distribution graph of gray-level values of Fig. 7B indicates that the gray-level values of CsPbBr₃@PVA sensor array reached stable after 5 s.

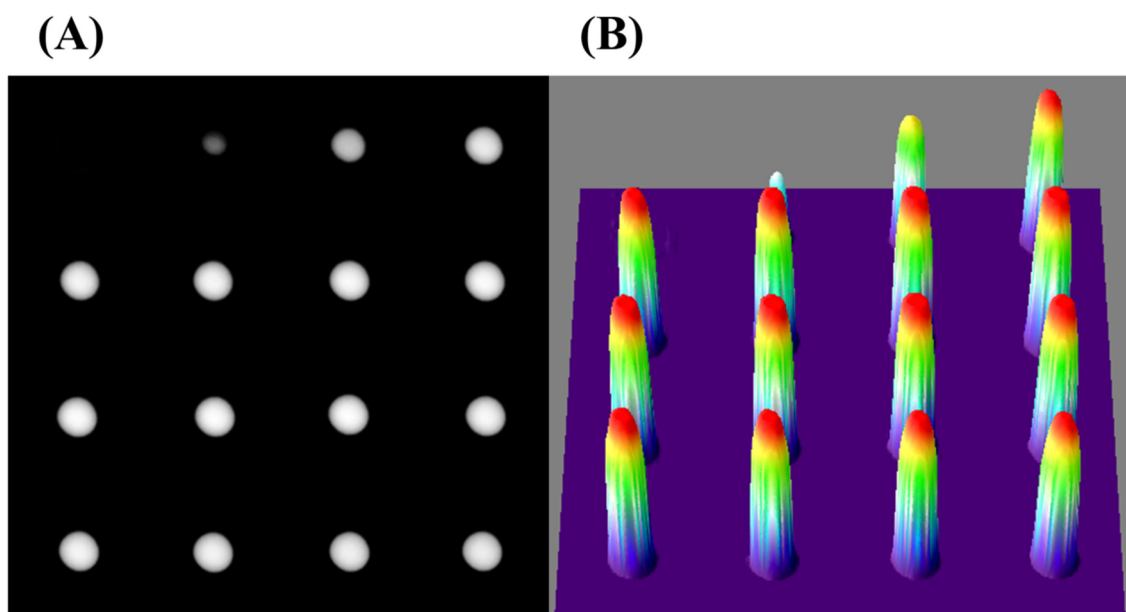


Figure S6. The gray-level image converted from fluorescence image by ImageJ (A) and the corresponding 3D distribution graph of gray values (B).

In the experimental process, it is found that the concentration of PVA, the concentration of CsPbBr₃ in CsPbBr₃@PVA, the mixing time of CsPbBr₃ and PVA and the volume of anhydrous ethanol have great influence on the sensor performance.

Firstly, the concentration of PVA used was determined. It was found that the CsPbBr₃@PVA material prepared with the concentration of 8% PVA had the best comprehensive properties, such as the dispersion of CsPbBr₃, the recovery ability of anhydrous ethanol to quenched fluorescence, the viscosity of the dispersion system, and the stability of no stratification after a long mixing time.

Secondly, the content of CsPbBr₃ in CsPbBr₃@PVA, the mixing time of CsPbBr₃ and PVA and the volume of anhydrous ethanol were determined. As shown in Figure S7, gray-level analysis method was used to study the fluorescence recovery degree under different conditions. The larger the value of G/G_0 is, the higher the fluorescence recovery degree is. In Figure S7A, it can be seen that the ratio of fluorescence intensity is the highest at 6% when CsPbBr₃ content varied from 3% to 7%. The 6% CsPbBr₃ content of CsPbBr₃@PVA can achieve the best response to anhydrous ethanol with the same mixing time and as little amount of CsPbBr₃ as possible. Therefore, CsPbBr₃@PVA with 6% CsPbBr₃ content was selected. As shown in Figure S7B, the fluorescence recovery degree of anhydrous ethanol to CsPbBr₃@PVA at different mixing time was explored. At 8 h, 16 h and 24 h after physical mixing CsPbBr₃ and PVA, the fluorescence of CsPbBr₃ was not completely quenched, so the background value G_0 was high and the response to anhydrous ethanol was not sensitive enough. At 32 h after physical mixing CsPbBr₃ and PVA, the fluorescence of CsPbBr₃ was almost quenched. At this time, the G/G_0 value reached the highest within the shortest material preparation time. Therefore, CsPbBr₃@PVA with the mixing time of 32 h was selected. As shown in Figure S7C, it is found that when the dropping amount of anhydrous ethanol is 4 μ L, the sensor response reaches the maximum with the minimum amount of ethanol, and this volume of anhydrous ethanol can completely infiltrate CsPbBr₃@PVA film after diffusion, so 4 μ L is selected as the best amount of anhydrous ethanol.

Thirdly, 0.015 g CsPbBr₃@PVA was found to be able to exactly cover the black opaque wafer with a size of 1 cm, so 0.015 g was selected.

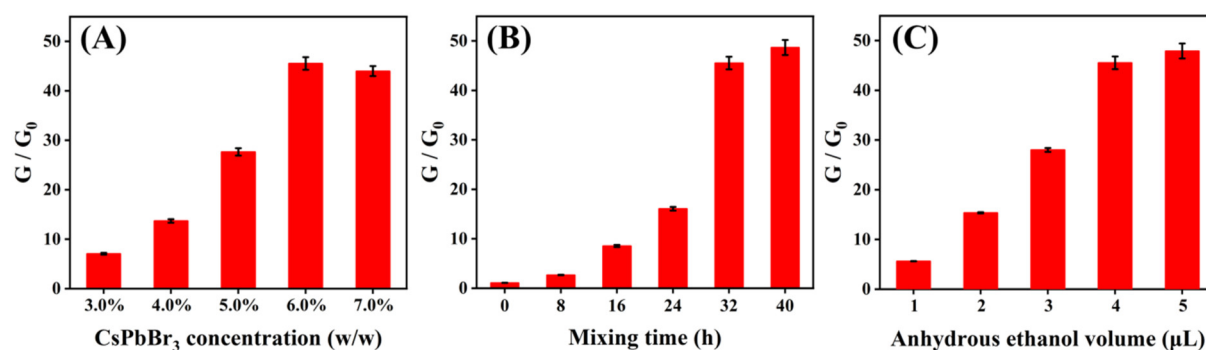


Figure S7. Conditions optimization for the water content detection: CsPbBr₃ concentration in CsPbBr₃@PVA (A), mixing time of CsPbBr₃ and PVA (B), volume of anhydrous ethanol (C). G channel has significant gray-level peaks in contrast to B and R channels.

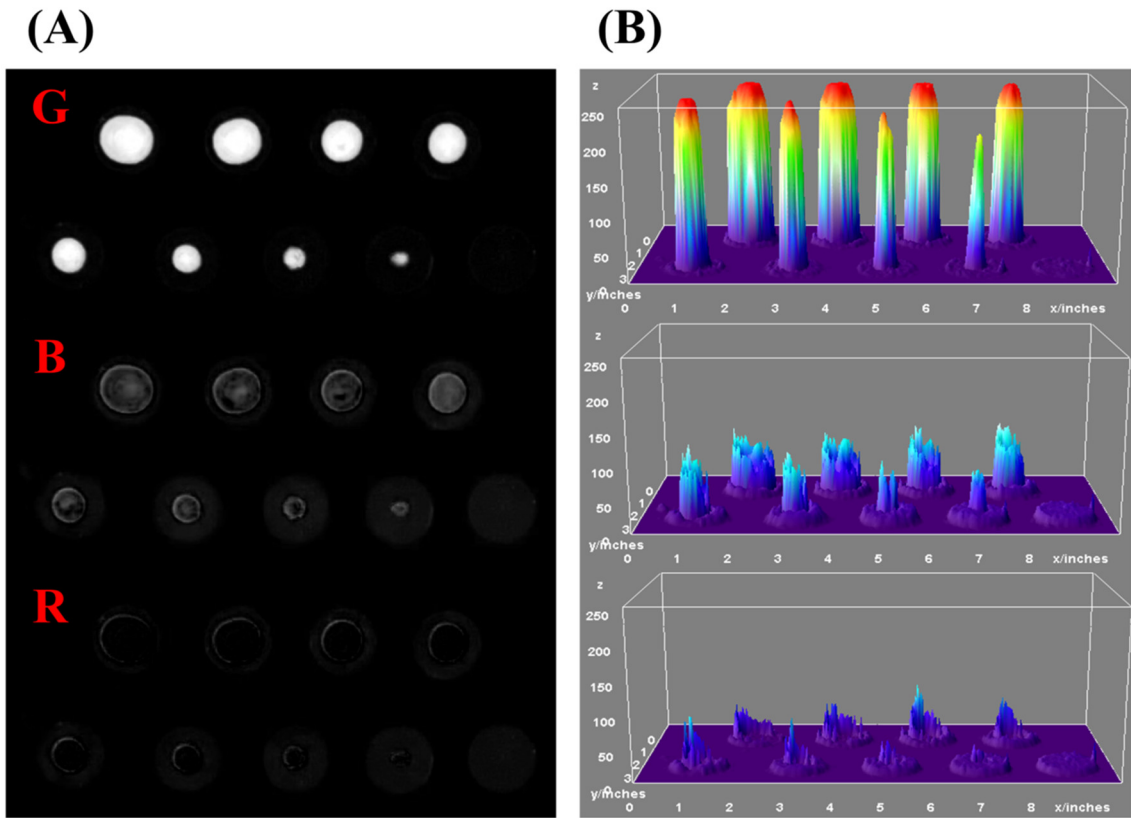


Figure S8. The gray-level images of green, blue and red channels, respectively (A); the corresponding 3D distribution graphs of gray values from (A) (B).

It could be seen that G values decreased significantly with the increase of water content while the R and B values stayed constant.

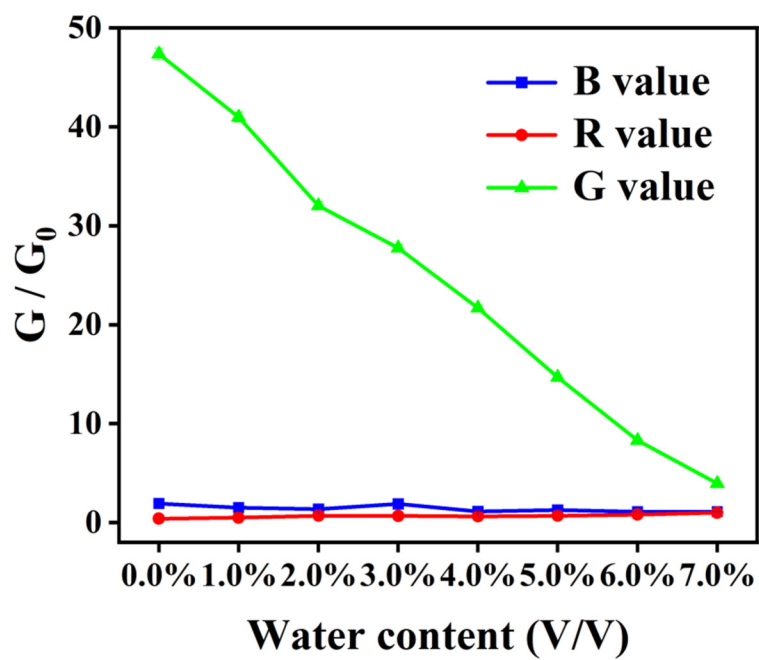


Figure S9. The gray ratio G/G_0 change of green, blue and red values of sensor array.

Smartphone iPhone 12, iPhone X and Xiaomi 8 were used to take fluorescence images of sensor array. Different mobile phone brands (Apple and Xiaomi) had an effect on the absolute value of gray-level values, but little effect on the relative value G/G_0 . The same brand but different models (iPhone 12 and iPhone X) had little effect on the results as well.

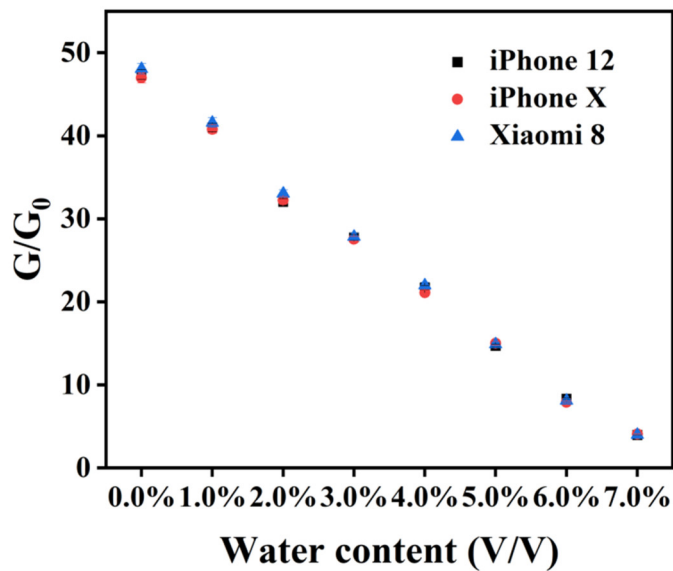


Figure S10. The relationship between gray ratio G/G_0 and water contents obtained by iPhone 12, iPhone X and Xiaomi 8.

CsPbBr₃@PVA sensor array can be preserved for at least a week with stable fluorescence recovery ability. As shown in the top of Figure S11, the Q CsPbBr₃@PVA film stored in the indoor dark environment for 1 week still did not have fluorescence recovery. In the bottom of Figure S11, 4 μL anhydrous ethanol was added to freshly prepared Q CsPbBr₃@PVA and Q CsPbBr₃@PVA stored 1 week, and it was observed that similar fluorescence recovery area and intensity of the two films. This is because the moisture in Q CsPbBr₃@PVA film is difficult to volatilize in the indoor environment due to the presence of a large number of hydrophilic hydroxyl groups, and the fluorescence of CsPbBr₃@PVA sensor array is difficult to recover naturally.

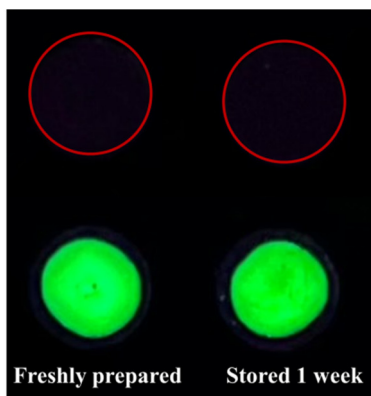


Figure S11. Comparison of fluorescence recovery ability of freshly prepared and stored for 1 week of CsPbBr₃@PVA sensors.

The decay curves of F CsPbBr₃@PVA and R CsPbBr₃@PVA were fitted by biexponential function: $I = A_1 \times \exp(-t/t_1) + A_2 \times \exp(-t/t_2)$, where $I = y - y_0$, $t = x$, A_1 and A_2 are weighted coefficients, t_1 and t_2 represent respectively the decay time of the fast and slow components of PL. The related coefficients of the double exponential function are listed as follows.

Table S1. Analysis of decay curves by using a biexponential fit: average lifetimes.

	R CsPbBr ₃ @PVA	F CsPbBr ₃ @PVA
A_1	1038.26	2079.39
t_1	26.06	1.63
A_2	437.10	803.51
t_2	275.93	11.02